

RESEARCH ARTICLE

Open Access

# The tubulin cofactor A is involved in hyphal growth, conidiation and cold sensitivity in *Fusarium asiaticum*

Xiaoping Zhang<sup>1</sup>, Xiang Chen<sup>1</sup>, Jinhua Jiang<sup>2</sup>, Menghao Yu<sup>1</sup>, Yanni Yin<sup>1\*</sup> and Zhonghua Ma<sup>1</sup>

## Abstract

**Background:** Tubulin cofactor A (TBCA), one of the members of tubulin cofactors, is of great importance in microtubule functions through participating in the folding of  $\alpha/\beta$ -tubulin heterodimers in *Saccharomyces cerevisiae*. However, little is known about the roles of TBCA in filamentous fungi.

**Results:** In this study, we characterized a TBCA orthologue FaTBCA in *Fusarium asiaticum*. The deletion of *FaTBCA* caused dramatically reduced mycelial growth and abnormal conidiation. The *FaTBCA* deletion mutant ( $\Delta$ FaTBCA-3) showed increased sensitivity to low temperatures and even lost the ability of growth at 4°C. Microscopic observation found that hyphae of  $\Delta$ FaTBCA-3 exhibited blebbing phenotypes after shifting from 25 to 4°C for 1- or 3-day incubation and approximately 72% enlarged nodes contained several nuclei after 3-day incubation at 4°C. However, hyphae of the wild type incubated at 4°C were phenotypically indistinguishable from those incubated at 25°C. These results indicate that *FaTBCA* is involved in cell division under cold stress (4°C) in *F. asiaticum*. Unexpectedly,  $\Delta$ FaTBCA-3 did not exhibit increased sensitivity to the anti-microtubule drug carbendazim although quantitative real-time assays showed that the expression of *FaTBCA* was up-regulated after treatment with carbendazim. In addition, pathogenicity assays showed that  $\Delta$ FaTBCA-3 exhibited decreased virulence on wheat head and on non-host tomato.

**Conclusion:** Taken together, results of this study indicate that FaTBCA plays crucial roles in vegetative growth, conidiation, temperature sensitivity and virulence in *F. asiaticum*.

**Keywords:** TBCA, Conidiation, Cold sensitivity, *F. asiaticum*, Hyphal growth, Fusarium head blight

## Background

Microtubules polymerized by  $\alpha/\beta$ -tubulin heterodimers play a central role in many cellular processes, including cell divisions, intracellular transport processes, and cell polarity. Biosynthesis of tubulin heterodimers is a multi-step process involving several molecular chaperones and tubulin cofactors (TBCs) [1]. In *Saccharomyces cerevisiae*, the nascent  $\alpha$ - and  $\beta$ -tubulin polypeptides firstly interact with prefoldin and cytosolic chaperonin CCT (Cytosolic-Chaperonin-containing-TCP1) [2]. Subsequently, five TBCs (TBCA-E) participate in the tubulin folding pathway. TBCA and TBCB bind to  $\beta$ -tubulin and  $\alpha$ -tubulin, respectively, which then transfer  $\beta$ -tubulin to

TBCD and  $\alpha$ -tubulin to TBCE respectively [3,4]. Afterwards, TBCC binds to the supercomplex containing TBCD, TBCE,  $\alpha$ - and  $\beta$ -tubulin, and stimulates GTP hydrolysis resulting in the release of the  $\alpha/\beta$ -tubulin heterodimers [5].

TBCA, as a  $\beta$ -tubulin-interacting protein, was first purified from bovine testis [6]. To date, characterization of several TBCA in yeast, murine, Arabidopsis and human has demonstrated that TBCA regulates both the ratio between  $\alpha$ - and  $\beta$ -tubulin and the tubulin folding pathways for correct polymerization into microtubules [7-11]. Rbl2p, the TBCA yeast orthologue, is not an essential gene in *S. cerevisiae* but is required for normal meiosis [7]. In fission yeast *Schizosaccharomyces pombe*, TBCA orthologue Alp31 plays an important role in the maintenance of microtubule integrity and the determination of the cell polarity [11]. Mutations in *KIS* (TBCA

\* Correspondence: ynyin@zju.edu.cn

<sup>1</sup>Institute of Biotechnology, Zhejiang University, Hangzhou, China  
Full list of author information is available at the end of the article

orthologue) lead to defects similar to the phenotypes associated with impaired microtubule function in *Arabidopsis* [9]. TBCA knockdown by RNAi in human cell lines, results in decreased amounts of  $\alpha$ - and  $\beta$ -tubulin levels, subtle alterations in the microtubule cytoskeleton, G1 cell cycle arrest and cell death [10].

*Fusarium asiaticum* (teleomorph: *Gibberella zeae*) is one of major causal agents that are responsible for economically important Fusarium head blight (FHB) on various cereal crops [12-15]. In addition to yield reduction, this pathogen produces mycotoxins including deoxynivalenol (DON), acetyldeoxynivalenol (3-ADON or 15-ADON), nivalenol (NIV), and acetylnivalenol (4-ANIV) in infected plants, which pose a serious threat to human and animal health [16,17]. In China, *F. asiaticum* is more important than *F. graminearum* with respect to population quantity and mycotoxin production [15]. Because highly resistant wheat cultivars are not available [18], chemical control remains one of the major strategies for the management of FHB [19]. However, highly effective fungicides against FHB are limited [19]. Moreover, *Fusarium* spp. have developed resistance to several commercialized fungicides [20-23]. Therefore, the exploration of new compounds and potential targets is desperately needed for an effective management of FHB. In the therapies of human diseases, TBCA has been regarded as an attractive target for the treatment of clear cell renal cell carcinoma (ccRCC), since it plays crucial roles in the progression, invasion and metastasis of ccRCC [24]. Until now, little is known about the roles of TBCA in filamentous fungi. In this study, we were thus interested in investigating the functions of TBCA in *F. asiaticum*, which may help in its exploitation as a drug target for the design of new antifungal agents against FHB.

## Methods

### Strains and culture conditions

*F. asiaticum* strain GJ33 collected from Jiangsu province, China was used as a wild-type strain in this study. The wild-type strain and the resulting transformants were grown on potato dextrose agar (PDA; 200 g potato, 20 g dextrose, 20 g agar and 1 l water), complete medium (CM; 1% glucose, 0.2% peptone, 0.1% yeast extract, 0.1% casamino acids, nitrate salts, trace elements, 0.01% vitamins and 1 l water, pH 6.5), minimal medium (MM; 10 mM  $K_2HPO_4$ , 10 mM  $KH_2PO_4$ , 4 mM  $(NH_4)_2SO_4$ , 2.5 mM NaCl, 2 mM  $MgSO_4$ , 0.45 mM  $CaCl_2$ , 9 mM  $FeSO_4$ , 10 mM glucose and 1 l water, pH 6.9), or wheat-head medium (200 g grounded fresh wheat heads and 20 g agar in 1 l water) for mycelial growth tests, and in carboxymethyl cellulose liquid medium (CMC; 15 g carboxymethyl cellulose, 1 g yeast extract, 0.5 g  $MgSO_4$ , 1 g  $NH_4NO_3$ , 1 g  $KH_2PO_4$  and 1 l water), or mung bean

agar (MBA; 40 g mung beans boiled in 1 l water for 20 min, and then filtered through cheesecloth, 20 g agar) for sporulation tests.

### Sequence analysis of *FaTBCA* gene from *F. asiaticum*

Based on the sequence of *TBCA* (FGSG\_00510.3) gene in *F. graminearum*, one pair of primers A1 + A2 (Additional file 1) was designated to amplify *FaTBCA* from GJ33 DNA. PCR amplifications were purified, cloned, and sequenced. The sequence of *FaTBCA* was deposited in GenBank under accession number KM116518. On the basis of deduced amino acid sequences of *FaTBCA* and its orthologues, the phylogenetic tree was generated by the neighbor-joining method with 1000 bootstrap replicates using the Mega 4.1 software [25].

### Yeast complementation assays

Full-length cDNA of *FaTBCA* was amplified using primer pair A3 + A4 listed in Additional file 1. PCR product was digested with appropriate enzymes and cloned into the pYES2 vector (Invitrogen Co., CA, USA), and transformed into the corresponding yeast mutant. Yeast transformants were then selected on synthetic medium lacking uracil. Additionally, the wild-type strain BY4741 and the mutant transformed with an empty pYES2 vector were used as controls. For complementation assays, the yeast transformants were grown at 30°C on YPRG medium (1% yeast extract, 2% bactopectone, 2% galactose) supplied with 0.48% (v/v) HCl. The experiments were repeated three times independently. There are four replicates for each experiment.

### Construction of gene deletion and complemented strains

*FaTBCA* deletion vector pBS-*FaTBCA*-Del was constructed by inserting two flanking sequences of *FaTBCA* into left and right sides of *HPH* (hygromycin resistance gene) in the pBS-*HPH1* vector [26]. Briefly, by using primer pair A5 + A6 (Additional file 1), a 477 bp upstream flanking sequence of *FaTBCA* was amplified from GJ33 genomic DNA, and was inserted into *XhoI-SalI* sites of the pBS-*HPH1* vector to generate a plasmid pBS-*FaTBCA*-Up. Subsequently, a 417 bp downstream flanking sequence of *FaTBCA* amplified from GJ33 genomic DNA using the primers A7 + A8 (Additional file 1) was inserted into *HindIII-BamHI* sites of the pBS-*FaTBCA*-Up vector to generate a plasmid pBS-*FaTBCA*-Del. Finally, the 2394 bp fragment containing *FaTBCA*-upstream-*HPH*-*FaTBCA*-downstream cassette was obtained by PCR amplification with primer pair A5 + A8 from the pBS-*FaTBCA*-Del. The resultant PCR product was purified and used for protoplast transformation. The PEG-mediated protoplast fungal transformation was performed as described previously [27]. For selective

growth of transformants, PDA medium supplemented with hygromycin ( $100 \text{ mg l}^{-1}$ ) were used.

To confirm that the phenotype of *FaTBCA* deletion mutant is due to disruption of the gene, genetic complementation was performed. The *FaTBCA* complement plasmid pCA-*FaTBCA*-Com was constructed using the backbone of pCAMBIA1300. First, a *XhoI-KpnI neo* cassette containing a *trpC* promoter was amplified from plasmid pBS-RP-Red-A8-NEO [28] with primers Neo-F + Neo-R (Additional file 1), and cloned into the *XhoI-KpnI* site of pCAMBIA1300 to create plasmid pCA-*neo*. Then, a 1862 bp of full length *FaTBCA* gene including 1437 bp promoter region was amplified using primer pair A11 + A12 (Additional file 1) from genomic DNA of the wild-type GJ33, and subsequently cloned into the *KpnI-XbaI* sites of pCAMBIA1300 to generate the complement plasmid pCA-*FaTBCA*-Com. Transformation of  $\Delta$ *FaTBCA*-3 with the full-length *FaTBCA* was conducted as described above except that geneticin ( $100 \text{ mg l}^{-1}$ ) was used as a selection agent. After single spore isolation, all of the mutants generated in this study were preserved in 15% glycerol at  $-80^\circ\text{C}$ .

#### Microscopic examinations of hyphal and conidial morphology

Hyphal growth of each strain was tested on PDA, CM, MM and wheat-head media at  $25^\circ\text{C}$  for 3 days. The experiment was repeated three times, and each with two replicates. Hyphal morphology was examined under a Nikon ECLIPSE Ni-U microscope (Nikon Co., Tokyo, Japan) from mycelia that were incubated in potato dextrose broth (PDB; 200 g potato, 20 g dextrose and 1 l water) at  $25^\circ\text{C}$  for 1 day using a shaker then transferred to static incubation at 4, 10 and  $25^\circ\text{C}$  for 1 day or 3 days. Furthermore, nucleus of hyphae were examined under the same microscope after staining with 4',6-diamidino-2-phenylindole (DAPI), as described previously [29]. The experiments were repeated three times independently. A total of 150 hyphae were examined for each strain.

For conidiation assays, two methods were used. One method used was to count spores produced in CMC liquid media, using fresh mycelia (50 mg) of each strain taken from the edge of a 3-day-old colony to inoculate 100 ml of CMC liquid media. The flasks were incubated at  $25^\circ\text{C}$  for 5 days in a shaker (180 rpm). The other method used was to count spores produced on MBA, using  $2 \mu\text{l}$  of a  $1 \times 10^6 \text{ ml}^{-1}$  spore suspension to inoculate a MBA plate. After one week of incubation, two ml of water was added to the plate and spread over the mycelium to collect spores. The amount of conidia was counted with a hemacytometer. The experiments were repeated three times independently. There are three replicates for each experiment.

Additionally, conidia of each strain were re-suspended in 2% (w/v) sucrose solutions and incubated at  $25^\circ\text{C}$  for 4 hrs, then conidial germination was examined under a Nikon ECLIPSE Ni-U microscope. Conidial morphology was observed under the same microscope. Furthermore, septum and nucleus were examined after staining conidia from each strain with calcofluor white (CFW) and DAPI, respectively, as described previously [29]. The experiments were repeated three times independently. A total of 150 conidia were examined for each strain.

#### Sensitivity determination to different stress agents

To determine the sensitivity to different temperatures, 5-mm mycelial plugs of each strain taken from 3-day-old colony edge were inoculated on PDA and then incubated at 4, 10, 15, 20, and  $25^\circ\text{C}$ . Three replicate plates for each temperature were used for each strain. After incubation for 3.5 days, colony diameter in each plate was measured in two perpendicular directions with the original mycelial plug diameter (5 mm) subtracted from each measurement. For each plate, the average of the colony diameters was used for calculating the percentage of growth inhibition. The mycelium growth of each strain at  $25^\circ\text{C}$  was arbitrarily set as control. The experiment was repeated three times. There are two replicates for each experiment.

To determine the sensitivity to various stresses, 5-mm mycelial plugs of each strain taken from 3-day-old colony edge were inoculated on MM amended with antifungal compound carbendazim, tebuconazole, iprodione or fludioxonil, on fructose gelatin agar (FGA; 10 g fructose, 2 g gelatin, 1 g  $\text{KH}_2\text{PO}_4$ , 0.5 g  $\text{MgSO}_4 \cdot 7\text{H}_2\text{O}$ , 2 g  $\text{NaNO}_3$ , 20 g agar and 1 l water, pH 7.0) amended with antifungal compound pyrimethanil, or on MM amended with cell wall stress agent congo red or SDS, osmotic agent NaCl or sorbitol, oxidative stress generator  $\text{H}_2\text{O}_2$  or paraquat, or metal ion  $\text{CaCl}_2$  or  $\text{MnCl}_2$ . The fungicides described above were kindly provided by the Institute of Zhejiang Chemical Industry or the Institute for the Control of Agrochemicals, Ministry of Agriculture (ICAMA), Beijing, China. The concentration of each compound is presented in Additional file 2. After incubation for 3.5 days, colony diameter in each plate was measured in two perpendicular directions with the original mycelial plug diameter (5 mm) subtracted from each measurement. For each plate, the average of the colony diameters was used for calculating the percentage of growth inhibition. The experiment was repeated three times. There are two replicates for each experiment.

#### Pathogenicity assays on flowering wheat heads and tomatoes

Pathogenicity test was performed with single floret injection method as previously described [30]. After incubation

in CMC medium for 5 days, conidia of each strain were collected by filtration through three layers of gauze and subsequently resuspended in sterile distilled water to a concentration of  $1 \times 10^5$  conidia  $\text{ml}^{-1}$ . A 10- $\mu\text{l}$  aliquot of conidial suspension was injected into a floret in the central section spikelet of single flowering wheat heads of susceptible cultivar Jimai 22. There were ten replicates for each strain. After inoculation, the plants were kept at  $22 \pm 2^\circ\text{C}$  under 95–100% humidity with 12 hrs of daylight. Fifteen days after inoculation, the infected spikelets in each inoculated wheat head were recorded. The experiment was repeated four times. To examine the ability to colonize tomato, a 10- $\mu\text{l}$  aliquot of conidial suspension was injected into the wounded tomato after surface sterilization. There are five replicates for each strain. Inoculated tomatoes were incubated under the same conditions described above, and were photographed 3 days after inoculation. The experiment was repeated three times.

#### Determination of DON production

A 50-g aliquot of healthy wheat kernels was sterilized and inoculated with 50 mg fresh mycelia of each strain. After incubation at  $25^\circ\text{C}$  for 20 days, DON and fungal ergosterol were extracted using previously described protocols [31]. The DON extracts were purified with PuriToxSR DON column TC-T200 (Trilogy analytical laboratory), and amounts of DON and ergosterol in each sample were determined by using a HPLC system Waters 1525. The experiment was repeated three times, each with three replicates.

#### Analysis of gene expression

Total RNA of each strain was extracted using the TaKaRa RNAiso Reagent, and 10  $\mu\text{g}$  of each RNA sample was used for reverse transcription with the oligo(dT)<sub>18</sub> primer using a RevertAid H Minus First Strand cDNA Synthesis kit. Expression of each gene was determined by quantitative reverse-transcriptase PCR (RT-PCR) with the corresponding primer pair (Additional file 1). The RT-PCR amplifications were performed in a DNA Engine Opticons 4 System (MJ Research) using the SYBR Green I fluorescent dye detection. Amplifications were conducted in 20- $\mu\text{l}$  volumes containing 10  $\mu\text{l}$  SYBR<sup>®</sup> Premix Ex Taq (TaKaRa Biotechnology Co., Ltd, Dalian, China), 2  $\mu\text{l}$  template DNA and 1  $\mu\text{l}$  each 4  $\mu\text{M}$  primer (each primer pair per amplification). There were three replicates for each sample. The real-time PCR amplifications were performed with the following parameters: an initial preheat at  $95^\circ\text{C}$  for 2 min, followed by 35 cycles at  $95^\circ\text{C}$  for 15 s,  $58^\circ\text{C}$  for 20 s,  $72^\circ\text{C}$  for 20 s, and  $80^\circ\text{C}$  for 3 s in order to quantify the fluorescence at a temperature above the denaturation of primer-dimers. Once amplifications were completed, melting curves

were obtained to identify PCR products. For each sample, PCR amplifications with primer pair Actin-F + Actin-R (Additional file 1) for the quantification of expression of *ACTIN* gene were performed as a reference. The relative expression levels of each gene in each strain or under the treatment were calculated using the  $2^{-\Delta\Delta\text{Ct}}$  method [32]. The experiment was repeated three times.

#### Standard molecular methods

Fungal genomic DNA was extracted using a previous published protocol [33]. Plasmid DNA was isolated using a Plasmid Miniprep Purification Kit (BioDev Co., Beijing, China). Southern analysis of *FaTBCA* gene in *F. asiaticum* was performed using probe as indicated in Additional file 3. The probe was labeled with digoxigenin (DIG) using a High Prime DNA Labeling and Detection Starter kit II according to the manufacturer's instructions (Roche Diagnostics; Mannheim, Germany).

#### Statistical analysis

All data for gene expression, DON production, conidiation and conidial germination were subjected in an analysis of variance (ANOVA) and the means were separated using Fisher's protected least significant difference ( $P = 0.05$ ). In the sensitivity to environmental stresses assays, the mycelial growth inhibition of  $\Delta\text{FaTBCA-3}$  under each stress was compared with that of the wild type using a *t* test.

## Results

#### *In silico* analysis of *FaTBCA* in *F. asiaticum*

One tubulin binding cofactor A (TBCA) (FGSG\_00510.3) was retrieved by BLASTP searching the *F. graminearum* genome database (<http://www.broadinstitute.org>) with the *S. cerevisiae* TBCA orthologue Rbl2 as a query. Based on the DNA sequences of FGSG\_00510.3, the corresponding orthologue *FaTBCA* was amplified and sequenced from *F. asiaticum*. Sequencing analysis showed that the nucleotide sequence of *FaTBCA* is 425 bp in length including one predicted intron, and is predicted to encode a 119 amino-acid protein. Phylogenetic analyses showed that *FaTBCA* is homologous to their counterparts from other filamentous fungi and yeast (Additional file 4). In addition, protein domain analysis by Pfam (<http://pfam.xfam.org/>) revealed that *FaTBCA* contains a conserved TBCA domain (Additional file 4). However, the deduced amino acid sequence of TBCA from the wild-type GJ33 is not highly homologous to those from other fungi (Additional file 4). For example, the deduced amino acid sequence of TBCA in GJ33 shared 46.0, 37.7 and 30.3% identity to those from *Magnaporthe oryzae* (MagoCoA, XP\_003709983.1), *Aspergillus nidulans* (AnCoA, CBF70033.1) and *S. cerevisiae* (SaCoA, EGA72990.1), respectively.

### FaTBCA partially complement the yeast $\Delta Rb12$ mutant

To characterize the functions of *FaTBCA*, we first tested whether this gene could complement an HCl-sensitive *S. cerevisiae* *TBCA* mutant ( $\Delta Rb12$ ) whose growth is dramatically inhibited on YPRG amended with 0.48% (v/v) HCl. An expression vector pYES2 containing the full-length *FaTBCA* cDNA was transferred into  $\Delta Rb12$ . As a negative control, the mutant was also transformed with an empty pYES2 vector. As shown in Figure 1, the reduced growth of yeast  $\Delta Rb12$  on YPRG +0.48% HCl was partially restored by *F. asiaticum* *FaTBCA*. These results indicate that *FaTBCA* could function as a *TBCA* in *S. cerevisiae*.

### Deletion and complementation of *FaTBCA* in *F. asiaticum*

To investigate the function of *FaTBCA*, we generated gene deletion mutants using a homologous recombination strategy (Additional file 3). Seven deletion mutants were identified from 13 hygromycin-resistant transformants by PCR analysis with the primer pair A9 + A10 (Additional file 1). The primer pair amplified 1710 and 460 bp fragments from *FaTBCA* deletion mutants and the wild-type progenitor GJ33, respectively. All seven deletion mutants showed identical growth defects on PDA plates. When probed with a 973 bp upstream DNA fragment of *FaTBCA*, the deletion mutant  $\Delta FaTBCA-3$  had an anticipated 5315 bp band, but lacked a 2205 bp band which was present in the wild-type GJ33 (Additional file 3). This Southern hybridization pattern confirmed that the transformant  $\Delta FaTBCA-3$  is a null mutant resulting from expected homologous recombination events at the *FaTBCA* locus. The complemented strain  $\Delta FaTBCA-3C$  was a single copy of *FaTBCA* inserted into the genome of  $\Delta FaTBCA-3$  (Additional file 3).

### Involvement of *FaTBCA* in vegetative growth and conidiation in *F. asiaticum*

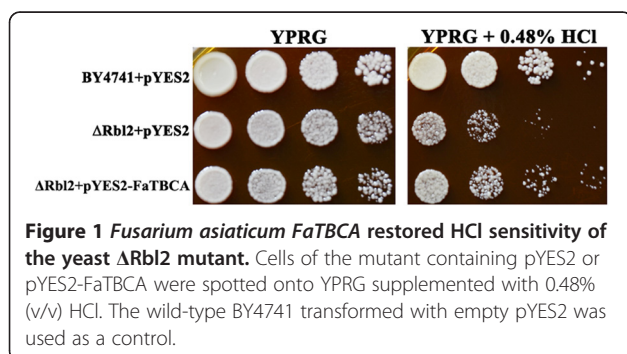
The *FaTBCA* deletion mutant  $\Delta FaTBCA-3$  grew significantly slower than the wild-type GJ33 on PDA, CM, MM and wheat-head media (Figure 2). Compared to the wild-type GJ33,  $\Delta FaTBCA-3$  produced a similar number

of conidia (Additional file 5), however, conidia of  $\Delta FaTBCA-3$  were shorter and with less septa (Figure 3A and B). Microscopic examination showed that 81.7% of  $\Delta FaTBCA-3$  conidia had one to three septa with conidial lengths ranging from 23.6 to 57.7  $\mu\text{m}$  (Figure 3A, C and D). In contrast, 62.6% of the wild-type conidia had four or five septa, with lengths ranging from 62.7 to 80.4  $\mu\text{m}$  (Figure 3A, C and D). In addition, conidial germination assays found that conidia of  $\Delta FaTBCA-3$  did not show delayed germination (Additional file 5).

### The *FaTBCA* deletion mutant showed increased sensitivity to low temperatures

Previous studies have reported that cold temperatures have disruptive effects on the stability of microtubules [34,35], we therefore determined the sensitivity of the *FaTBCA* deletion mutant to low temperatures. As shown in Figure 4A and B, the inhibition percentages of mycelial growth of the mutant  $\Delta FaTBCA-3$  at 10, 15 and 20°C were significantly higher than those of the wild type. Furthermore, after 7 days of incubation at 4°C, the wild type exhibited an obvious growth, however,  $\Delta FaTBCA-3$  did not show any sign of growth (Figure 4C). After 21 days of incubation at 4°C, the colony diameter of the wild type was greater than 5.8 cm, whereas, the  $\Delta FaTBCA-3$  mutant was still unable to grow (Figure 4C), indicating that the deletion of *FaTBCA* caused the stagnation of growth at 4°C. The  $\Delta FaTBCA-3$  mutant restored growth after shifting from 4 to 25°C (data not shown).

In order to explore why the mutant  $\Delta FaTBCA-3$  cannot grow at the cold temperature 4°C, we further observed the hyphal morphology and nuclear distribution of  $\Delta FaTBCA-3$  after 1-day or 3-day incubation at 4°C. After incubation in a shaker at 25°C for 1 day, the wild type and  $\Delta FaTBCA-3$  were immediately transferred to 4°C for 1 or 3 days. Microscopic observation showed that the hyphal tips of  $\Delta FaTBCA-3$  began to present blebbing phenotypes after 1-day incubation at 4°C (Figure 5). Moreover, the enlarged nodes occurred not only in hyphal tips but also in hyphal middle sections after 3-day incubation (Figure 5). By observing 150 hyphal tips, we found that 9 and 83% hyphal tips showed bulged nodes after 1 and 3 days of incubation at 4°C, respectively. Furthermore, 4',6-diamidino-2-phenylindole (DAPI) staining assays showed that approximately 72% enlarged nodes contained several nuclei by counting 100 enlarged nodes (Figure 6). However, the hyphal morphology and nuclear distribution of the wild type after incubation at 4°C exhibited no obvious difference compared to those after incubation at 10 or 25°C (Figure 5, 6 and Additional file 6). Taken together, these results indicate that *FaTBCA* plays a critical role in the cell division under cold stress (4°C) in *F. asiaticum*.



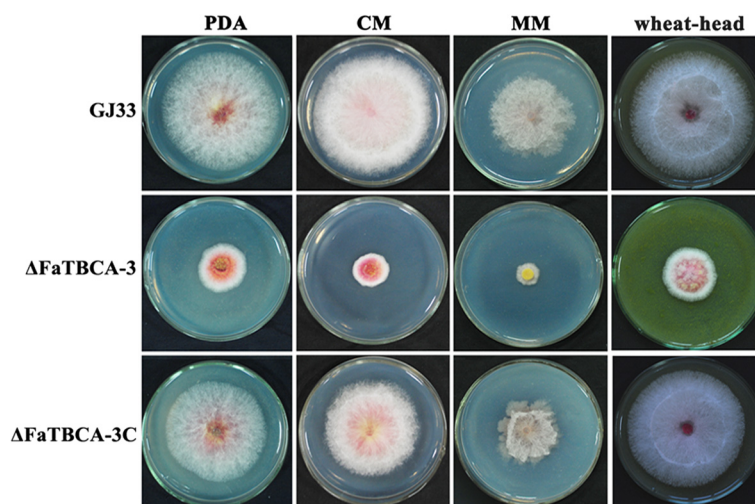


**Figure 2 Impact of *FaTBCA* deletion on *F. asiaticum* hyphal growth.** The wild-type GJ33,  $\Delta FaTBCA-3$  and  $\Delta FaTBCA-3C$  were grown on solid media, PDA, CM, MM and wheat-head at 25°C for 3 days.

#### The deletion of *FaTBCA* did not change the sensitivity to carbendazim

Since the fungicide carbendazim can cause the depolymerization of fungal microtubules, we tested the sensitivity of the mutant to this compound. Surprisingly,  $\Delta FaTBCA-3$  did not differ from the wild type in carbendazim sensitivity, as well as in other fungicides including tebuconazole, iprodione, fludioxonil and pyrimethanil (Additional file 2). In addition, the deletion of *FaTBCA* had no effect on the sensitivity of *F. asiaticum* to cell wall damaging agents, and to osmotic, oxidative and metal cation stresses (Additional file 2).

Given that the *FaTBCA* deletion mutant  $\Delta FaTBCA-3$  did not show increased sensitivity to carbendazim, we were interested in the expression of *FaTBCA* treated with carbendazim and the expression of two  $\alpha$ -tubulin genes (encoded by *FaTUA1* and *FaTUA2*) in  $\Delta FaTBCA-3$  mutant. As shown in Additional file 7, the expression of *FaTBCA* increased 3.1 times under the treatment of  $3.5 \mu\text{g ml}^{-1}$  carbendazim. Quantitative real-time PCR analysis showed that the expression of *FaTUA1* and *FaTUA2* in  $\Delta FaTBCA-3$  showed no significant difference compared with the wild-type GJ33 (Additional file 7), indicating that there might be other unknown genes involved in regulating the balance of the  $\alpha/\beta$ -tubulin monomers.

#### *FaTBCA* is required for full virulence and DON biosynthesis in *F. asiaticum*

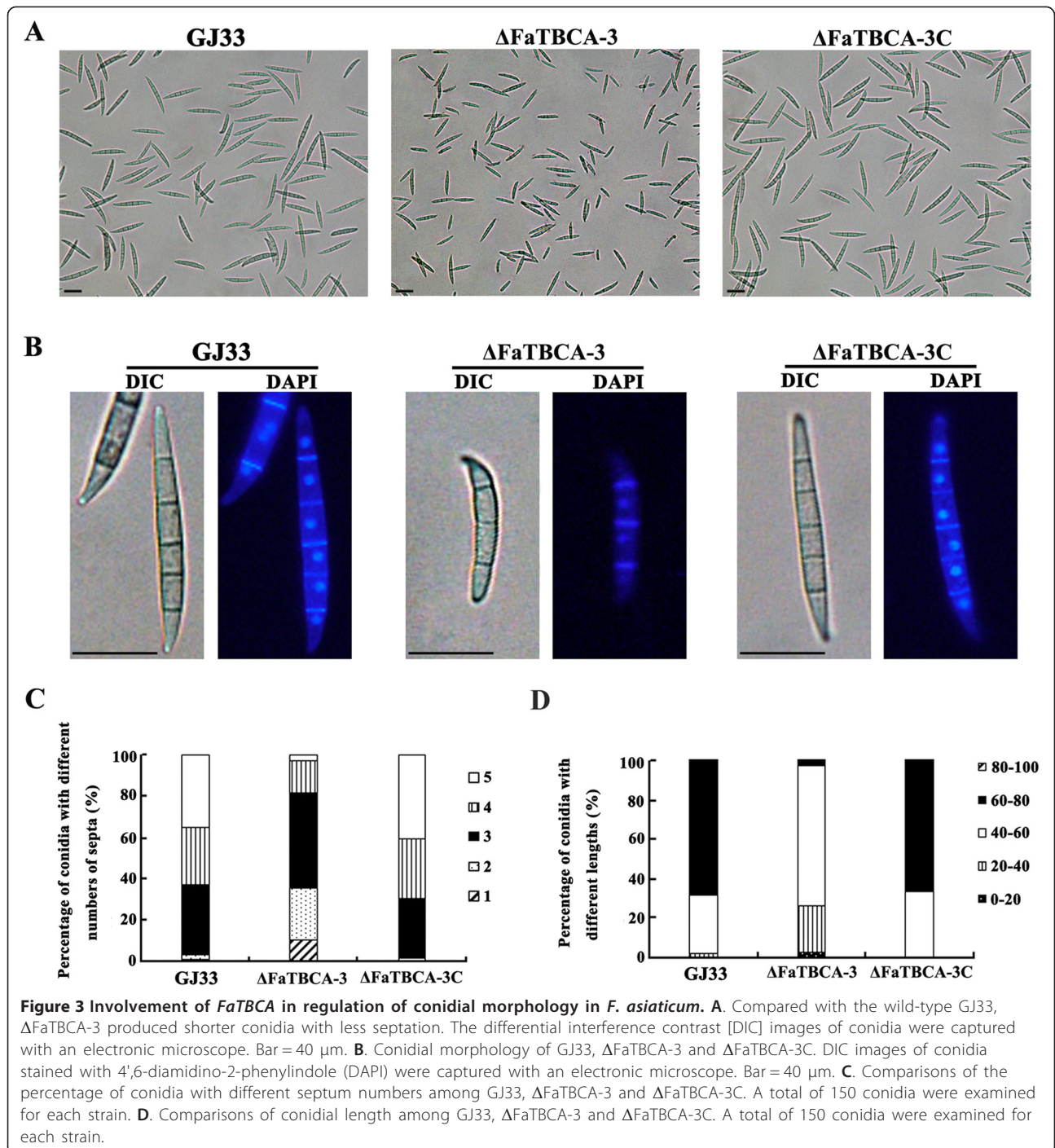
Pathogenicity assays indicated that disruption of *FaTBCA* caused a significant reduction in the virulence of *F. asiaticum*. As shown in Figure 7A, the wild-type strain GJ33 and  $\Delta FaTBCA-3C$  caused the typical scab symptoms in

the inoculated and nearby spikelets of flowering wheat heads 15 days after inoculation. Under the same conditions, however, scab symptoms caused by  $\Delta FaTBCA-3$  were only observed in the inoculated spikelet and in the adjacent two or three spikelets. Furthermore, three days after inoculation of non-host tomatoes, the water-soaked rot lesion caused by  $\Delta FaTBCA-3$  was significantly smaller than that caused by GJ33 or  $\Delta FaTBCA-3C$  (Figure 7B).

Previous studies have shown that DON is an important virulence factor and a prerequisite for colonization of wheat [36,37]. Therefore, we were interested in the effect of *FaTBCA* deletion on DON biosynthesis. After growth on sterilized wheat kernels for 20 days, the amount of DON produced by the wild type was 6.2 folds higher than that produced by  $\Delta FaTBCA$  (Figure 7C). To further confirm the results, we determined the expression levels of *TRI6* and *TRI10* by quantitative real-time PCR using RNA samples isolated from mycelia grown in minimal synthetic liquid medium (MS) [38] for 4 days at 25°C. The expression levels of *TRI6* and *TRI10* in  $\Delta FaTBCA$  reduced by 94% and 76%, respectively, as compared to those in the wild type (Figure 7D). These results indicate that *FaTBCA* plays a critical role in DON biosynthesis in *F. asiaticum*.

#### Discussion

In this study, we characterized a putative tubulin cofactor A *FaTBCA*, a homologue of *S. cerevisiae* Rbl2 in *F. asiaticum*. Although *FaTBCA* shares low homology with similar proteins found in other organisms, *F. asiaticum* *FaTBCA* can restore the sensitivity to HCl of the *RBL2* deletion mutant of budding yeast. Similarly, expression



of mouse *TBCA* not only suppresses the benomyl supersensitivity resulting from the deletion of *RBL2* in *S. cerevisiae* [7], but also rescues all defects of a *KIS* (*TBCA* orthologue) mutant under the control of the 35S promoter in *Arabidopsis* [9]. The protein sequence of mouse *TBCA* is approximately 30% and 35% identical to *Rbl2* and *Kis*, respectively. Therefore, the functions of

*TBCA* homologues from yeast to higher eukaryotic organisms are evolutionally conserved.

Although *TBCA* in eukaryotic organisms are conserved, the detailed roles of *TBCAs* among different species are not fully consistent. In this present study, the deletion of *FaTBCA* leads to reduced vegetative growth and abnormal conidia with less septation in *F. asiaticum*

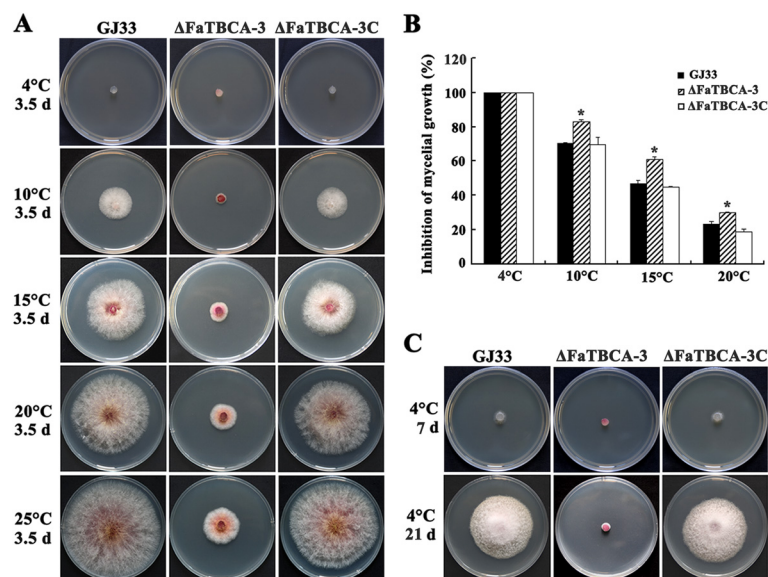


**Figure 4** The deletion of *FaTBCA* increased sensitivity to low temperatures. **A**. Mycelial plugs of the wild-type GJ33,  $\Delta FaTBCA-3$  and  $\Delta FaTBCA-3C$  were inoculated on PDA and incubated at 4, 10, 15, 20 and 25°C for 3.5 days. **B**. Inhibition percentages of mycelial growth of GJ33,  $\Delta FaTBCA-3$  and  $\Delta FaTBCA-3C$  at 4, 10, 15 and 20°C. After incubation for 3.5 days, colony diameter in each plate was measured in two perpendicular directions with the original mycelial plug diameter (5 mm) subtracted from each measurement. For each plate, the average of the colony diameters was used for calculating the percentage of growth inhibition. The mycelium growth of each strain at 25°C was arbitrarily set as control. Line bars in each column denote standard errors of three experiments. \* = significant difference for each temperature at a 95% coincidence interval by performing a t test. **C**. The mutant  $\Delta FaTBCA-3$  was unable to grow at 4°C after incubation for 7 or 21 days.

(Figures 2 and 3), which is not in agreement with the situations in yeast. In *S. cerevisiae* and *S. pombe*, TBCA homologues are dispensable for cell growth and asexual development, but played important roles in meiosis and growth polarity, respectively. Previous studies on *F. asiaticum* reported that the deletion of each  $\beta$ -tubulin results in reduced vegetative growth, abnormal conidial morphology or decreased conidiation [21,39,40]. Our *FaTBCA* deletion mutant  $\Delta FaTBCA-3$  shared similar phenotypes with  $\beta$ -tubulin disruption mutants of *F. asiaticum*, indicating that TBCA in *F. asiaticum* is involved in the maintenance of microtubule function as reported in other eukaryotic organisms.

Microtubules are dynamic by nature, with an equilibrium existing between soluble subunits and the polymerized filament that could influence normal cellular functions. Previous studies have found that low temperature generally shifts this equilibrium toward depolymerization and leads to intrinsic cold sensitivity of microtubule [34,35]. In this study, we found that the deletion of *FaTBCA* increased the sensitivity to low temperatures in *F. asiaticum* (Figure 4A and B), indicating that deletion of *FaTBCA* might accelerate the depolymerization of microtubule at low temperatures. However, a precise monitoring of microtubule dynamics under cold stress would have to be addressed to confirm this hypothesis.

Under the cold temperature 4°C, the *FaTBCA* mutant exhibited growth stagnation accompanied with the phenotype of several nuclei in the enlarged hyphal nodes (Figures 5 and 6), indicating that *FaTBCA* is involved in cell division. This might be a major contributor to the stagnation of growth at 4°C. In Arabidopsis, mesophyll cells in leaf sections of *KIS* mutant frequently were highly enlarged and the enlarged cells had one large nucleus or several nuclei [9]. In human HeLa cells transfected with TBCA siRNA also exhibits blebbing phenotypes, which are considered to be due to the changes of microtubule structures [10]. Taken together, our results showed that the TBCA in *F. asiaticum* might share some functions with Kis in Arabidopsis [9].

Carbendazim and other benzimidazole fungicides, which target  $\beta$ -tubulin and interrupt the polymerization of microtubules, have been extensively used to control various plant diseases caused by fungi [40]. The treatment of anti-microtubule drug carbendazim caused the up-regulation of *FaTBCA* in *F. asiaticum* (Additional file 7), which supported that TBCA serves as a reservoir of excess  $\beta$ -tubulin [1,8]. To our surprise, unlike the case in *S. cerevisiae* [7], the absence of *FaTBCA* did not render cells more sensitive to carbendazim (Additional file 2). In budding yeast, over-expression of either Rbl2 or  $\alpha$ -tubulin suppresses  $\beta$ -tubulin lethality and causes



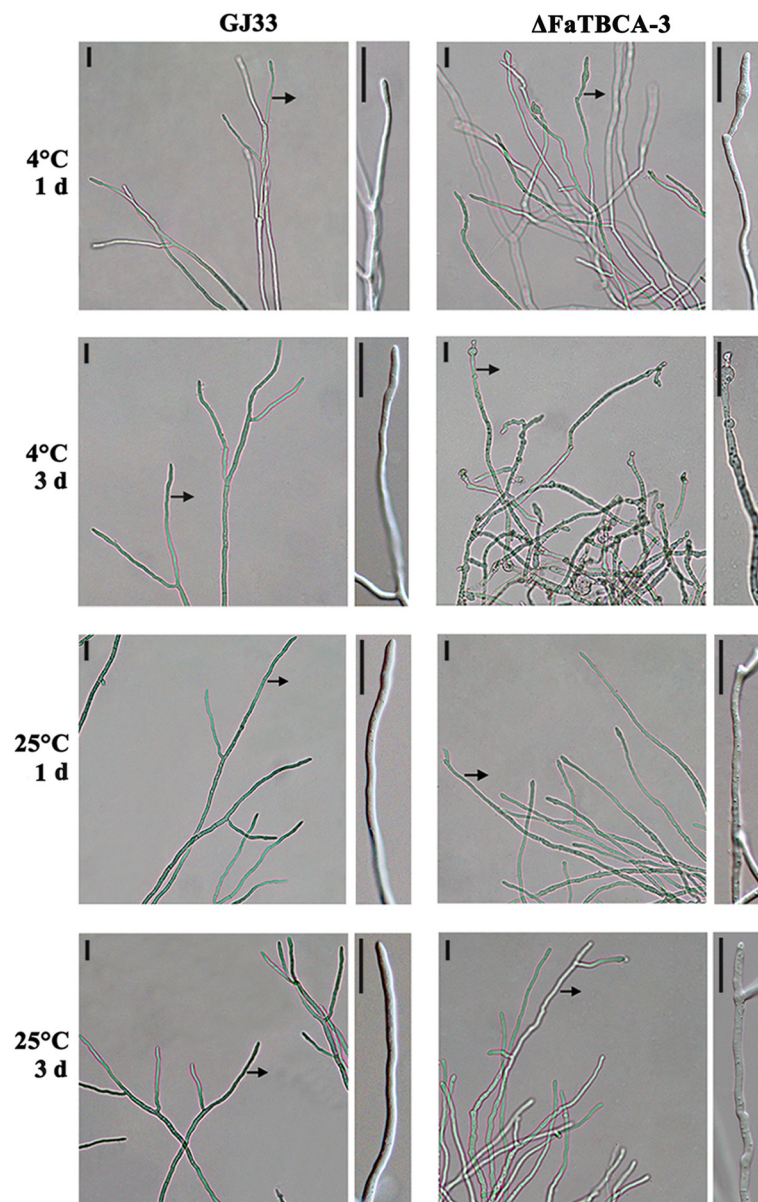


**Figure 5 Hyphae of  $\Delta$ FaTBCA-3 exhibit blebbing phenotypes under cold stress.** Differential interference contrast [DIC] images of hyphae were captured with an electronic microscope. Bar = 100  $\mu$ m. The enlarged hyphae are indicated by black arrows. The wild-type GJ33 and  $\Delta$ FaTBCA-3 were incubated in PDB at 25°C for 1 day with a shaker then transferred to static incubation at 4 and 25°C for 1 or 3 days.

resistance to antimicrotubule drug benomyl [7]. However, our quantitative real-time PCR assays found that the deletion of *FaTBCA* did not result in significant change in the expression levels of two  $\alpha$ -tubulin genes (Additional file 7), indicating that there might be other unknown genes involved in the control of the  $\alpha/\beta$ -tubulin monomer balance.

In addition to the involvement of *FaTBCA* in regulating mycelial growth, conidiation and low temperature

sensitivity, this gene is also required for virulence of *F. asiaticum*. The reduced virulence in  $\Delta$ FaTBCA may result from three defects of the mutant. First,  $\Delta$ FaTBCA showed drastic mycelium growth defect, which might be a major contributor. As observed on PDA, the mutant also grew significantly slower than the wild-type strain on the wheat-head medium (Figure 2). Second, the ability of  $\Delta$ FaTBCA to produce trichothecene mycotoxins in infected wheat kernels was greatly decreased.

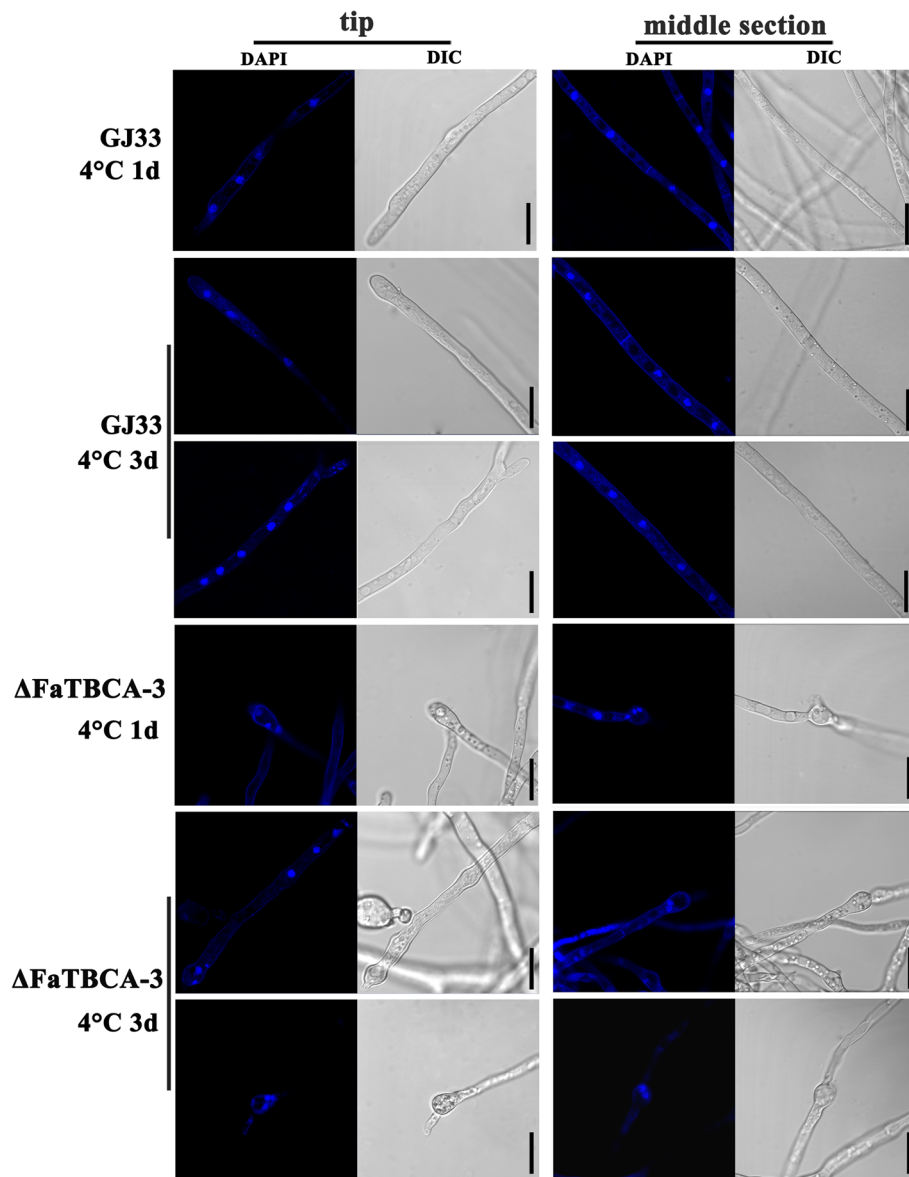


**Figure 6** The number of nuclei in  $\Delta$ FaTBCA-3 increases under cold stress. Differential interference contrast [DIC] images of nuclei in hyphal tip and middle section of the wild-type GJ33 and  $\Delta$ FaTBCA-3 were taken after staining with 4',6-diamidino-2-phenylindole (DAPI). Bar = 10  $\mu$ m. Each strain was incubated in PDB at 25°C for 1 day with a shaker then transferred to static incubation at 4°C for 1 or 3 days.

DON, the end product of the trichothecene biosynthetic pathway, plays an important role in the spread of FHB within a spike [36,37], thus this may also contribute to the reduced virulence of the mutant. Third, TBCA has been found to play a crucial role in correct polymerization of microtubules [7,9]. Moreover, previous studies have reported that extracellular secretion of virulence factors is dependent on microtubule-mediated vesicle transport in pathogenic fungi [41-43]. Thus, the reduced virulence in  $\Delta$ FaTBCA-3 might be

associated with the disturbance of microtubule-dependent vesicle transport.

### Conclusion

Our *FaTBCA* studies in *F. asiaticum* found that *FaTBCA* plays critical roles in vegetative growth, conidial morphology, sensitivity to low temperatures and virulence. To our knowledge, this is the first report about the functions of TBCA in filamentous fungi. Our results indicate that

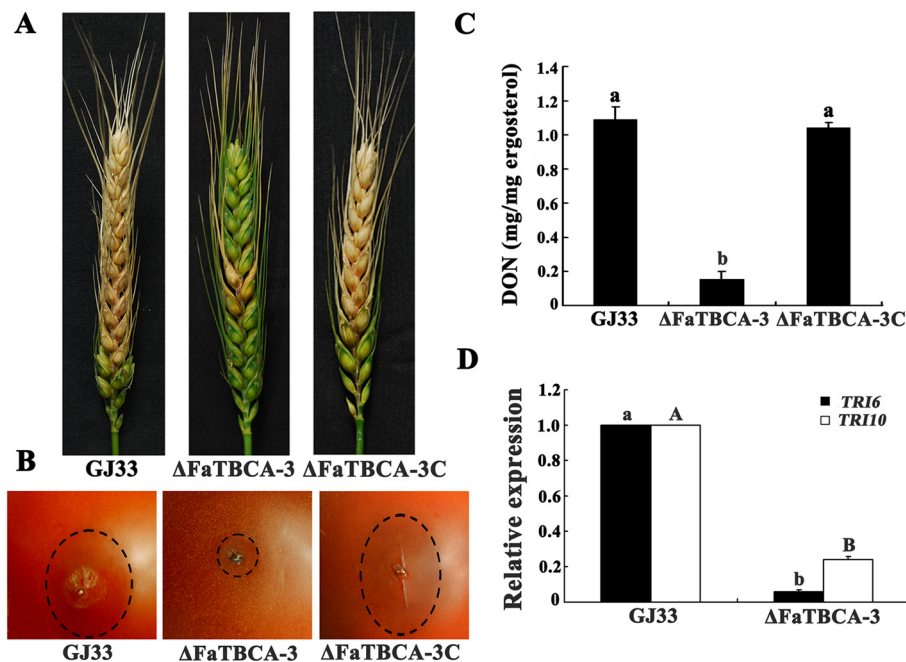


**Figure 7** *FaTBCA* is required for full virulence and DON biosynthesis in *F. asiaticum*. **A.** Flowering wheat heads were point inoculated with a conidial suspension at  $10^5$  conidia  $\text{ml}^{-1}$  of the wild-type GJ33,  $\Delta\text{FaTBCA-3}$  and  $\Delta\text{FaTBCA-3C}$ , and infected wheat heads were photographed 15 days after inoculation. **B.** Tomatoes were inoculated with a conidial suspension at  $10^5$  conidia  $\text{ml}^{-1}$  of each strain and infected fruits were photographed 3 days after inoculation. **C.** The amount of DON (per mg fungal ergosterol) produced by each strain in infected wheat kernels was determined after 20 days of inoculation. Line bars in each column denote standard errors of three experiments. Values on the black bars followed by the same letter are not significantly different according to a Fisher's least significant difference (LSD) test at  $P=0.05$ . **D.** Relative expression of DON biosynthetic *TRI* genes in each strain and bars denote standard errors from three experiments. Values on the black bars followed by the same letter for each gene are not significantly different according to a Fisher's least significant difference (LSD) test at  $P=0.05$ .

the functions of *TBCA* in *F. asiaticum* are partially different from what have reported in yeast.

## Additional files

**Additional file 1:** Oligonucleotide primers used in this study.

**Additional file 2:** Sensitivity of GJ33,  $\Delta\text{FaTBCA-3}$  and  $\Delta\text{FaTBCA-3C}$  to environmental stresses. **A.** Comparisons were made on MM plates amended with  $10 \mu\text{g ml}^{-1}$  iprodione,  $0.25 \mu\text{g ml}^{-1}$  tebuconazole,  $0.5 \mu\text{g ml}^{-1}$  carbendazim,  $0.05 \mu\text{g ml}^{-1}$  rapamycin,  $0.25 \text{ M CaCl}_2$ ,  $10 \mu\text{g ml}^{-1}$  paraquat,  $0.05\% \text{ H}_2\text{O}_2$ ,  $0.7 \text{ M NaCl}$ ,  $0.7 \text{ M sorbitol}$ ,  $0.01\% \text{ SDS}$ , and  $0.2 \text{ g l}^{-1}$  congo red. **B.** Inhibition percentages of mycelial growth of GJ33,  $\Delta\text{FaTBCA-3}$  and  $\Delta\text{FaTBCA-3C}$  under each stress. After incubation for 3.5 days, colony diameter in each plate was measured in two perpendicular directions with the original mycelial plug diameter (5 mm) subtracted from each measurement. For each plate, the average of the colony diameters was used for calculating the percentage of growth inhibition. Line bars in each column denote standard errors of three experiments. A *t* test was performed to determine significant differences, \* = significant difference for each stress at a 95% coincidence interval.

**Additional file 3:** Generation and identification of *FaTBCA* gene deletion mutant. **A.** Target gene *FaTBCA* deletion strategy. The hygromycin resistance cassette (*HPH*) is denoted by the large gray arrow. Primer binding sites are indicated by arrows (see Additional file 1 for the primer sequences). **B.** DNA hybridization analysis of the wild-type strain GJ33, *FaTBCA* deletion mutant  $\Delta\text{FaTBCA-3}$ , and the complemented transformant  $\Delta\text{FaTBCA-3C}$ , using a 973 bp *FaTBCA* fragment as a probe. Genomic DNA of each strain was digested with *HindIII*.

**Additional file 4:** **A.** Phylogenetic analysis of tubulin cofactor A (*TBCA*) orthologues from *Fusarium asiaticum* (*FaTBCA*, KM116518; indicated in the black boxes), *F. graminearum* (*FgTBCA*, FGSG\_00510.3), *F. pseudograminearum* (*FpTBCA*, EKJ75396.1), *F. verticillioides* (*FvTBCA*, EWG37294.1), *F. fujikuroi* (*FfTBCA*, CCT62423.1), *F. oxysporum* (*FoTBCA*, EWY93729.1), *Claviceps purpurea* (*CpTBCA*, CCE31346.1), *Colletotrichum graminicola* (*CgTBCA*, EFQ26205.1), *Co. orbiculare* (*CoTBCA*, ENH78242.1), *Verticillium dahliae* (*VdTBCA*, EGY18367.1), *Togninia minima* (*TmTBCA*, XP\_007910919.1), *Neurospora crassa* (*NcTBCA*, XP\_964483.1), *Magnaporthe oryzae* (*MoTBCA*, XP\_003709983.1), *Gaeumannomyces graminis* (*GgTBCA*, EJT76136.1), *Marssonina brunnea* (*Mb510*, XP\_007289220.1), *Blumeria graminis* (*BgTBCA*, CCU76202.1), *Neofusicoccum parvum* (*NpTBCA*, XP\_007583539.1), *Aspergillus nidulans* (*AnTBCA*, CBF70033.1), *Candida albicans* (*CaTBCA*, EEQ43562.1), *Saccharomyces cerevisiae* (*ScRbl2*, EGA72990.1), and *Schizosaccharomyces pombe* (*SpAlp3*, CAB40194.1). The phylogenetic tree was generated by the neighbor-joining method with 1000 bootstrap replicates using the Mega 4.1 software. **B.** Each *TBCA* orthologue contains one functional domain, tubulin binding cofactor A, which were identified by Pfam (<http://pfam.xfam.org/>). **C.** Alignment of the predicted amino acid sequences of *TBCA* domains from *F. asiaticum*, *M. oryzae*, *N. crassa*, *A. nidulans*, *S. cerevisiae*, *S. pombe*, and *C. albicans*. The Boxshade program was used to highlight identical (black shading) or similar (grey shading) amino acids.

**Additional file 5:** Effect of *FaTBCA* deletion on conidiation and conidium germination of *F. asiaticum*. **A.** Conidia were counted after incubation of the wild-type GJ33, the mutant  $\Delta\text{FaTBCA-3}$  and the complemented strain  $\Delta\text{FaTBCA-3C}$  in carboxymethyl cellulose liquid medium (CMC) for 5 days in a shaker at  $25^\circ\text{C}$ . **B.** Conidia were counted after incubation of each strain on mung bean agar (MBA) for one week

of incubation at 25°C. C. Conidia of each strain were incubated in 2% (w/v) sucrose solutions and incubated at 25°C for 4 hrs. After incubation for 4 hrs, conidium germination of 150 conidia was examined. Line bars in each column denote standard errors of three repeated experiments. Bars with the same letter indicate no significant difference according to a Fisher's least significant difference (LSD) test at  $P = 0.05$ .

**Additional file 6: The number of nuclei in  $\Delta$ FaTBCA-3 does not change after incubation at 10 or 25°C.** DIC images of nuclei in hyphal tip and middle section of the wild-type GJ33 and  $\Delta$ FaTBCA-3 were taken after staining with 4',6-diamidino-2-phenylindole (DAPI). Bar = 10  $\mu$ m. Each strain was incubated in PDB at 25°C for 1 day with a shaker then transferred to static incubation at 10 or 25°C for 3 days.

**Additional file 7: The relative expression levels of FaTBCA treated with 3.5  $\mu$ g ml<sup>-1</sup> anti-microtubule drug carbendazim (A), FaTUA1 and FaTUA2 in the FaTBCA deletion mutant  $\Delta$ FaTBCA-3 (B).** Line bars in each column denote standard errors of three experiments. Values on the black bars followed by the same letter for each gene are not significantly different according to a Fisher's least significant difference (LSD) test at  $P = 0.05$ .

### Competing interests

The authors declare that they have no competing interests.

### Authors' contributions

XZ performed most part of the experimental work. XC, JJ and MY determined the DON production and analyzed the results. YY designed and coordinated the study, participated in analysis of the results and wrote the manuscript. ZM helped in writing the manuscript. All authors read and approved the final version.

### Acknowledgements

This research was supported by the 973 Project (2013CB127802), National Science Foundation (31170135), and China Agriculture Research System (CARS-3-1-15).

### Author details

<sup>1</sup>Institute of Biotechnology, Zhejiang University, Hangzhou, China. <sup>2</sup>Institute of Agriculture Quality and Standard for Agro-products, Zhejiang Academy of Agricultural Sciences, Hangzhou, China.

Received: 16 October 2014 Accepted: 4 February 2015

Published online: 18 February 2015

### References

- Lopez-Fanarraga M, Avila J, Guasch A, Coll M, Zabala JC. Review: postchaperonin tubulin folding cofactors and their role in microtubule dynamics. *J Struct Biol.* 2001;135:219–29.
- Vainberg IE, Lewis SA, Rommelaere H, Ampe C, Vandekerckhove J, Klein HL, et al. Prefoldin, a chaperone that delivers unfolded proteins to cytosolic chaperonin. *Cell.* 1998;93:863–73.
- Lewis SA, Tian G, Cowan NJ. The  $\alpha$ - and  $\beta$ -tubulin folding pathways. *Trends Cell Biol.* 1997;7:479–84.
- Tian G, Lewis SA, Feierbach B, Stearns T, Rommelaere H, Ampe C, et al. Tubulin subunits exist in an activated conformational state generated and maintained by protein cofactors. *J Cell Biol.* 1997;138:821–32.
- Fontalba A, Paciucci R, Avila J, Zabala JC. Incorporation of tubulin subunits into dimers requires GTP hydrolysis. *J Cell Sci.* 1993;106:627–32.
- Gao Y, Melki R, Walden PD, Lewis SA, Ampe C, Rommelaere H, et al. A novel cochaperonin that modulates the ATPase activity of cytoplasmic chaperonin. *J Cell Biol.* 1994;125:989–96.
- Archer JE, Vega LR, Solomon F, Rbl2p, a yeast protein that binds to  $\beta$ -tubulin and participates in microtubule function in vivo. *Cell.* 1995;82:425–34.
- Fanarraga ML, Parraga M, Aloria K, del Mazo J, Avila J, Zabala JC. Regulated expression of p14 (cofactor A) during spermatogenesis. *Cell Motil Cytoskeleton.* 1999;43:243–54.
- Kirik V, Grini PE, Mathur J, Klinkhammer I, Adler K, Bechtold N, et al. The Arabidopsis tubulin-folding cofactor A gene is involved in the control of the  $\alpha/\beta$ -tubulin monomer balance. *Plant Cell.* 2002;14:2265–76.
- Nolasco S, Bellido J, Gonçalves J, Zabala JC, Soares H. Tubulin cofactor A gene silencing in mammalian cells induces changes in microtubule cytoskeleton, cell cycle arrest and cell death. *FEBS Lett.* 2005;579:3515–24.
- Radcliffe PA, Garcia MA, Toda T. The cofactor-dependent pathways for  $\alpha$ - and  $\beta$ -tubulins in microtubule biogenesis are functionally different in fission yeast. *Genetics.* 2000;156:93–103.
- Gale LR, Hernick CA, Takamura K, Chen LF, Kistler HC. Population analysis of *Fusarium graminearum* from wheat fields in eastern China. *Phytopathology.* 2002;92:1315–22.
- O'Donnell K, Ward TJ, Geiser DM, Kistler HC, Aoki T. Genealogical concordance between the mating type locus and seven other nuclear genes supports formal recognition of nine phylogenetically distinct species within the *Fusarium graminearum* clade. *Fungal Genet Biol.* 2004;41:600–23.
- Qu B, Li HP, Zhang JB, Xu YB, Huang T, Wu AB, et al. Geographical distribution and genetic diversity of the *Fusarium graminearum* and *F. asiaticum* on wheat spikes throughout China. *Plant Pathol.* 2008;57:15–24.
- Zhang JB, Li HP, Dang FJ, Qu B, Xu YB, Zhao CS, et al. Determination of the trichothecene mycotoxin chemotypes and associated geographical distribution and phylogenetic species of the *Fusarium graminearum* clade from China. *Myc Res.* 2007;111:967–75.
- McMullen M, Jones R, Gallenberg D. Scab of wheat and barley: a re-emerging disease of devastating impact. *Plant Dis.* 1997;81:1340–8.
- Pestka JJ, Smolinski AT. Deoxynivalenol: toxicology and potential effects on humans. *J Toxicol Environ Health B Crit Rev.* 2005;8:39–69.
- Goswami RS, Kistler HC. Heading for disaster: *Fusarium graminearum* on cereal crops. *Mol Plant Pathol.* 2004;5:515–25.
- Blandino M, Minelli L, Reyneri A. Strategies for the chemical control of Fusarium head blight: effect on yield, allelopathic parameters and deoxynivalenol contamination in winter wheat grain. *Eur J Agron.* 2006;25:193–201.
- Becher R, Hettwer U, Karlovsky P, Deising HB, Wirsig SGR. Adaptation of *Fusarium graminearum* to tebuconazole yielded descendants diverging for levels of fitness, fungicide resistance, virulence, and mycotoxin production. *Phytopathology.* 2010;100:444–53.
- Chen CJ, Yu JJ, Bi CW, Zhang YN, Xu JQ, Wang JX, et al. Mutations in a beta-tubulin confer resistance of *Gibberella zeae* to benzimidazole fungicides. *Phytopathology.* 2009;99:1403–11.
- Dubos T, Pasquali M, Pogoda F, Hoffmann L, Beyer M. Evidence for natural resistance towards trifloxystrobin in *Fusarium graminearum*. *Eur J Plant Pathol.* 2011;130:239–48.
- Yin YN, Liu X, Li B, Ma ZH. Characterization of sterol demethylation inhibitor-resistant isolates of *Fusarium asiaticum* and *F. graminearum* collected from wheat in China. *Phytopathology.* 2009;99:487–97.
- Zhang P, Ma X, Song E, Chen W, Pang H, Ni D, et al. Tubulin cofactor A functions as a novel positive regulator of cCRC progression, invasion and metastasis. *Int J Cancer.* 2013;133:2801–11.
- Kumar S, Nei M, Dudley J, Tamura K. MEGA: a biologist-centric software for evolutionary analysis of DNA and protein sequences. *Brief Bioinform.* 2008;9:299–306.
- Liu XH, Lu JP, Zhang L, Dong B, Min H, Lin FC. Involvement of a *Magnaporthe grisea* serine/threonine kinase gene *MgATG1* in appressorium turgor and pathogenesis. *Eukaryot Cell.* 2007;6:997–1005.
- Liu Z, Friesen TL. Polyethylene glycol (PEG)-mediated transformation in filamentous fungal pathogens. *Methods in Mol Bio.* 2012;835:365–75.
- Dong B, Liu XH, Lu JP, Zhang FS, Gao HM, Wang HK, et al. *MgAtg9* trafficking in *Magnaporthe oryzae*. *Autophagy.* 2009;5:946–53.
- Wang C, Zhang S, Hou R, Zhao Z, Zheng Q, Xu Q, et al. Functional analysis of the genome of the wheat scab fungus *Fusarium graminearum*. *Plos Pathog.* 2011;7:e1002460.
- Wu AB, Li HP, Zhao CS, Liao YC. Comparative pathogenicity of *Fusarium graminearum* isolates from China revealed by wheat coleoptile and floret inoculations. *Mycopathologia.* 2005;160:75–83.
- Mirocha CJ, Kolaczowski E, Xie W, Yu H, Jelen H. Analysis of deoxynivalenol and its derivatives (Batch and Single Kernel) using gas chromatography/mass spectrometry. *J Agric Food Chem.* 1998;46:1414–8.
- Livak KJ, Schmittgen TD. Analysis of relative gene expression data using real-time quantitative PCR and the  $2^{-\Delta\Delta Ct}$  Method. *Methods.* 2001;25:402–8.
- McDonald BA, Martinez JP. Restriction fragment length polymorphisms in *Septoria tritici* occur at high frequency. *Curr Genet.* 1990;17:133–8.
- Dawson PJ, Lloyd CW. Comparative biochemistry of plant and animal tubulins. In: Davies DD, editor. The biochemistry of plants. Volume 12th ed. New York: Academic; 1987. p. 3–47.

35. Fosket D. Cytoskeletal proteins and their genes in higher plants. In: The biochemistry of plants, vol. 15. New York: Academic; 1989. p. 393–454.
36. Proctor RH, Hohn TM, McCormick SP. Reduced virulence of *Gibberella zeae* caused by disruption of a trichothecene toxin biosynthetic gene. *Mol Plant Microbe In.* 1995;8:593–601.
37. Seong KY, Pasquali M, Zhou XY, Song J, Hilburn K, McCormick S, et al. Global gene regulation by *Fusarium* transcription factors *Tri6* and *Tri10* reveals adaptations for toxin biosynthesis. *Mol Microbiol.* 2009;72:354–67.
38. Merhej J, Boutigny AL, Pinson-Gadais L, Richard-Forget F, Barreau C. Acidic pH as a determinant of *TRI* gene expression and trichothecene B biosynthesis in *Fusarium graminearum*. *Food Addit Contam.* 2010;27:710–7.
39. Liu X, Yin YN, Wu JB, Jiang JH, Ma ZH. Identification and characterization of carbendazim-resistant isolates of *Gibberella zeae*. *Plant Dis.* 2010;94:1137–42.
40. Qiu JB, Xu JQ, Yu JJ, Bi CW, Chen CJ, Zhou MG. Localisation of the benzimidazole fungicide binding site of *Gibberella zeae*  $\beta$ -tubulin studied by site-directed mutagenesis. *Pest Manag Sci.* 2011;67:91–198.
41. Baravalle G, Schober D, Huber M, Bayer N, Murphy RF. Transferrin recycling and dextran transport to lysosomes is differentially affected by bafilomycin, nocodazole, and low temperature. *Cell Tissue Res.* 2005;320:99–113.
42. Chanda A, Roze LV, Kang S, Artymovich KA, Hicks GR. A key role for vesicles in fungal secondary metabolism. *Proc Natl Acad Sci U S A.* 2009;106:19533–8.
43. Conesa A, Punt PJ, van Luijk N, van den Hondel CAMJJ. The secretion pathway in filamentous fungi: a biotechnological view. *Fung Genet Biol.* 2001;33:155–71.

**Submit your next manuscript to BioMed Central and take full advantage of:**

- Convenient online submission
- Thorough peer review
- No space constraints or color figure charges
- Immediate publication on acceptance
- Inclusion in PubMed, CAS, Scopus and Google Scholar
- Research which is freely available for redistribution

Submit your manuscript at  
[www.biomedcentral.com/submit](http://www.biomedcentral.com/submit)

